

# Acquisition and Tracking of GIOVE-A Broadcast L1/E5/E6 Signals and Analysis of DME/TACAN Interference on Receiver Design

Grace Xingxin Gao, David S. De Lorenzo, Todd Walter and Per Enge  
Stanford University

## BIOGRAPHY

Grace Xingxin Gao is a Ph.D. candidate under the guidance of Professor Per Enge in the Electrical Engineering Department at Stanford University. She received a B.S. in Mechanical Engineering in 2001 and her M.S. in Electrical Engineering in 2003, at Tsinghua University, Beijing, China. Her current research interests include Galileo signal and code structures, GNSS receiver architectures, and GPS modernization.

David De Lorenzo is a member of the Stanford University GPS Laboratory, where he is pursuing a Ph.D. degree in Aeronautics and Astronautics. He received a Master of Science degree in Mechanical Engineering from the University of California, Davis, in 1996. David has worked previously for Lockheed Martin and for the Intel Corporation.

Todd Walter is a Senior Research Engineer in the Department of Aeronautics and Astronautics at Stanford University. Dr. Walter received his Ph.D. in 1993 from Stanford and is currently developing WAAS integrity algorithms and analyzing the availability of the WAAS signal. He is a fellow of the ION.

Per Enge is a Professor of Aeronautics and Astronautics at Stanford University, where he is the Kleiner-Perkins, Mayfield, Sequoia Capital Professor in the School of Engineering. He directs the GPS Research Laboratory, which develops satellite navigation systems based on the Global Positioning System (GPS). He has been involved in the development of WAAS and LAAS for the FAA. Per has received the Kepler, Thurlow and Burka Awards from the ION for his work. He is also a Fellow of the ION and the Institute of Electrical and Electronics Engineers (IEEE). He received his Ph.D. from the University of Illinois in 1983.

## ABSTRACT

This paper demonstrates the tracking and acquisition of GIOVE-A broadcast L1/E5/E6 signals of the Galileo system using a multi-signal all-in-view software receiver. We show that existing aeronautical systems interfere with the E5 signals and that interference mitigation at the receiver is necessary and effective for correct tracking.

The first test satellite of the Galileo system, GIOVE-A was launched on December 28, 2005 [1]. It started to broadcast Galileo signals on January 12th, 2006. GIOVE-A is capable of transmitting on two frequencies at one time from an available set of L1, E5 and E6 bands. Unlike its L1 and E6 counterparts, E5 signals at 1176.45 MHz and 1207.14 MHz are exposed to a unique electromagnetic environment created by existing aeronautical system pulsed emitters, specifically Distance Measuring Equipment (DME) and Tactical Air Navigation (TACAN) systems. DME provides a distance measurement between the aircraft and a ground station. TACAN is a military system that additionally provides azimuth information. These navigation systems consist of an airborne interrogator and a ground-based transponder. DME and TACAN operate in four modes (X, Y, W and Z) between 960 MHz and 1215 MHz. This range completely covers the E5a and E5b bands. Moreover, DME/TACAN from local airports have much greater signal strength than the GIOVE-A signal. The DME/TACAN interference dramatically degrades the signal-to-interference plus noise ratio (SINR), and makes the E5 signal processing more difficult than that of L1 and E6 signals.

Our previous papers [1] and [2] studied the signals and PRN sequences and code generators of the GIOVE-A transmission on L1, E5 and E6. In this paper, we implement the decoded PRN sequences and code generators into our multi-signal all-in-view Galileo software receiver. Broadcast signals are collected through a 1.8 meter dish antenna in the Stanford GNSS Monitoring System. We are able to acquire and track the broadcast GIOVE-A signals on all frequencies, L1, E5 and E6.

Acquisition is implemented as a parallel code-phase search using FFT-based processing. Several milliseconds of data may be combined to increase weak-signal sensitivity or to provide more accurate estimates of carrier Doppler frequency, although at a trade-off in execution time. Immediately after acquisition, the code-phase and carrier-frequency estimates are used to initialize the code and carrier numerically-controlled oscillators (NCOs). The receiver refines the estimates of carrier frequency, carrier phase, and code phase through a succession of tracking modes, where the phase-lock and delay-lock loop noise bandwidths are successively reduced.

In addition to acquisition and tracking, we also use the software receiver to study the DME interference in E5 band and analyze its effect on receiver design. We demonstrate that without any signal processing, the DME interference can cause phase and delay lock loop convergence failure. We solve this problem by applying pulse blanking to the raw signal before the acquisition module. Then the tracking loops converge consistently. Therefore, interference mitigation at receivers is necessary and effective for Galileo E5 signals.

Recently, China launched the first middle earth orbiting (MEO) satellite in its Compass GNSS system, 21,550 kilometres above the Earth. The satellite began transmitting signals on three frequencies within a few days. The transmitted signal was observed and the Pseudo Random Noise (PRN) code in the I-channel of E2 band has been decoded. The code generator of the Chinese Compass E2 signal is presented at the end of this paper.

## INTRODUCTION

The first test satellite of the Galileo system, GIOVE-A was launched on December 28, 2006. It is used to secure the Galileo frequencies allocated by the International Telecommunication Union (ITU) and also test certain Galileo satellite components [3]. GIOVE-A started to broadcast Galileo signals on January 12th, 2006. GIOVE-A is capable of transmitting on two frequencies at one time from an available set of L1, E5 and E6 bands as indicated in blue in the frequency allocation chart in Figure 1 [4]. It was first broadcasting on L1 and E6 bands. Based on our observation, it switched to L1 and E5 bands in August, 2006 for a few weeks and switched back to L1 and E6 frequencies in September, 2006. Since October 25, 2006, it has again been transmitting on L1 and E5 bands.

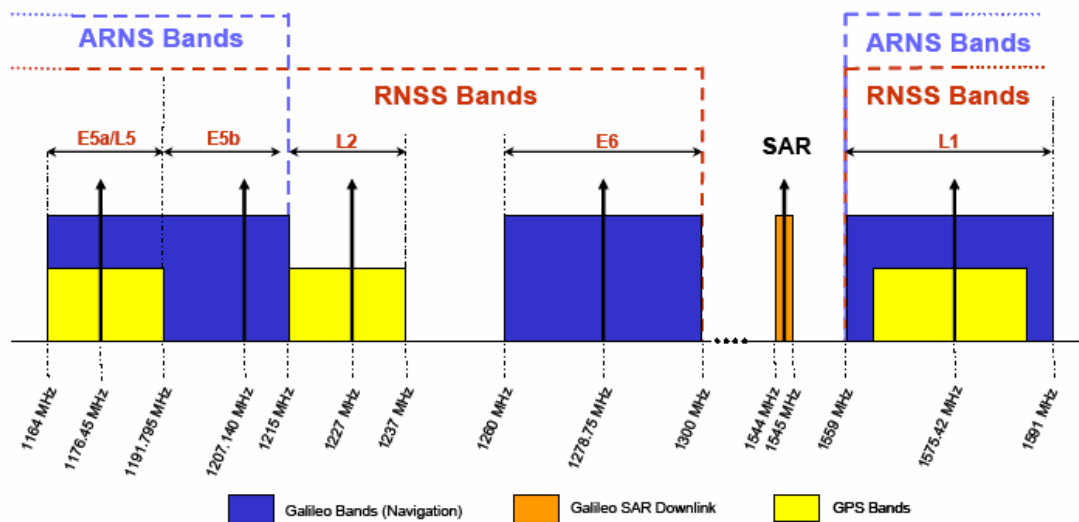


Figure 1. Galileo frequency allocation [4]

Unlike its L1 and E6 counterparts, E5 signals at 1176.45 MHz and 1207.14 MHz are exposed to strong interference created by existing aeronautical system pulsed emitters. DME provides distance measurement between aircraft and a ground station. TACAN is a military system. It provides not only the distance measurement, but also azimuth information. These navigation systems operate between 960 MHz and 1215 MHz in an Aeronautical Radionavigation Services (ARNS) band [5]. As shown in Figure 1, the ARNS band covers the E5 band and thus interfere with Galileo E5 signals. The DME/TACAN interference degrades the signal-to-interference plus noise ratio (SINR), and makes the E5 decoding process more difficult than decoding L1 and E6 codes.

## GIOVE-A SIGNALS AND PRN CODES

GIOVE-A is allocated with three frequency bands, L1, E5 and E6. The E5 band can be further divided into two subbands, E5a and E5b. In each frequency band or subband, there is at least one pilot channel with a secondary code modulated on the primary code and one data channel with navigation bits modulated on the primary code. The modulation type, primary code chip rate, symbol rate and power of each frequency band are listed in Table 1 [4].

Signal	Components	Modulation Type	Chip Rate (Mcps)	Sub Carrier Frequency (MHz)	Symbol Rate
L1	E1-A	BOC(15, 2.5)	2.5575	15.345	100
	E1-B data	BOC(1, 1)	1.023	1.023	250
	E1-C pilot				n/a
E5	E5a-I data	AltBOC(15, 10)	10.23	15.345	50
	E5a-Q pilot				N/A
	E5b-I data				250
	E5b-Q pilot				n/a
E6	E6-A	BOC (10, 5)	5.115	10.230	100
	E6-B data	BPSK(5)	5.115	n/a	1000
	E6-C pilot				n/a

Table 1. Primary GIOVE-A navigation signal parameters

Our previous papers [1] and [2] studied the signals and PRN sequences and code generators of the GIOVE-A transmission on L1, E5 and E6. We not only obtained the primary PRN code sequences of the transmitted signals, but also proved that all GIOVE-A broadcast codes are Gold codes and can be generated by linear feedback shift registers (LFSR). The code generator polynomials and initial states are listed in Table 2. Later on, the Galileo Open Service Signal In Space Interference Control Document (OS SIS ICD) [4] also disclose the codes, which confirmed our results.

L1-B code (4092 bits, 4msec, 13-stage Gold code)	
Polynomial_1	$X^{13}+X^{10}+X^9+X^7+X^5+X^4+1$
Initial State_1	[1 1 1 1 1 1 1 1 1 1 1 1 1]
Polynomial_2	$X^{13}+X^{12}+X^8+X^7+X^6+X^5+1$
Initial State_2	[1 1 0 1 1 1 0 0 0 0 1 1]
L1-C code (8184 bits, 8msec, 13-stage Gold code)	
Polynomial_1	$X^{13}+X^4+X^3+X+1$
Initial State_1	[1 1 1 1 1 1 1 1 1 1 1 1 1]
Polynomial_2	$X^{13}+X^{10}+X^9+X^7+X^5+X^4+1$
Initial State_2	[1 1 0 0 1 1 0 0 0 0 1 1]

a) L1 PRN codes

E6-B code (5115 bits, 1msec, 13-stage Gold code)	
Polynomial_1	$X^{13}+X^{10}+X^8+X^5+1$
Initial State_1	[1 1 1 1 1 1 1 1 1 1 1 1 1]
Polynomial_2	$X^{13}+X^{12}+X^{11}+X+1$
Initial State_2	[0 1 0 1 0 1 1 1 0 0 0 0]
E6-C code (10230 bits, 2msec, 14-stage Gold code)	
Polynomial_1	$X^{14}+X^{11}+X^6+X+1$
Initial State_1	[1 1 1 1 1 1 1 1 1 1 1 1 1 1]
Polynomial_2	$X^{14}+X^8+X^7+X^4+X^3+X^2+1$
Initial State_2	[0 1 1 0 1 0 0 0 0 1 1 1 0 1]

b) E6 PRN codes

E5a-I code (10230 bits, 1msec, 14-stage Gold code)	
Polynomial_1	$X^{14}+X^8+X^6+X+1$
Initial State_1	[1 1 1 1 1 1 1 1 1 1 1 1 1 1]
Polynomial_2	$X^{14}+X^{12}+X^8+X^7+X^5+X^4+1$
Initial State_2	[1 1 1 0 1 0 1 0 1 1 1 1 1 1]
E5a-Q code (10230 bits, 1msec, 14-stage Gold code)	
Polynomial_1	$X^{14}+X^8+X^6+X+1$
Initial State_1	[1 1 1 1 1 1 1 1 1 1 1 1 1 1]
Polynomial_2	$X^{14}+X^{12}+X^8+X^7+X^5+X^4+1$
Initial State_2	[0 1 1 0 1 1 0 0 1 0 1 0 1 0]

c) E5a PRN codes

E5b-I code (10230 bits, 1msec, 14-stage Gold code)	
Polynomial_1	$X^{14}+X^{13}+X^{11}+X^4+1$
Initial State_1	[1 1 1 1 1 1 1 1 1 1 1 1 1 1]
Polynomial_2	$X^{14}+X^{12}+X^9+X^8+X^5+X^2+1$
Initial State_2	[1 1 1 0 0 0 1 0 1 0 0 0 1 0]
E5b-Q code (10230 bits, 1msec, 14-stage Gold code)	
Polynomial_1	$X^{14}+X^{13}+X^{11}+X^4+1$
Initial State_1	[1 1 1 1 1 1 1 1 1 1 1 1 1 1]
Polynomial_2	$X^{14}+X^{12}+X^9+X^8+X^5+X^2+1$
Initial State_2	[1 1 0 0 0 0 0 0 0 0 1 0 0]

d) E5b PRN codes

Table 2. PRN codes of the broadcast GIOVE-A signals

## DATA COLLECTION

The GIOVE-A signals are collected by the Stanford SRI Dish and the Stanford GNSS Monitor Station (SGMS).

The Stanford SRI Dish shown in Figure 2, is a high gain parabolic antenna located in Stanford hills. It is 45.7 m in diameter, and the total structure weighs 1400000 kg. The surface is made of soft aluminum hex pattern mesh with 1.6

cm spacing. The SRI Dish is designed for L-band signals with central frequency 1420 MHz. Its attainable gain can be as high as 52 dB with  $0.25^\circ$  beamwidth and 35% efficiency.



Figure 2. Stanford SRI Dish



Figure 3. Stanford GNSS Monitor System, 1.8m dish

The other facility is SGMS, shown in Figure 3. SGMS has a 1.8 m steerable parabolic dish antenna with an L-band feed. The antenna has approximately  $7^\circ$  beamwidth, and provides about 25 dB of gain over conventional patch antennas. As the SGMS dish is located on the roof of the GPS Lab building, it is more accessible than the Stanford SRI Dish. In addition, the motor of the antenna can be driven by satellite tracking software, so that the dish can automatically point to and track a specific satellite.

The signal from the feed of the antenna goes through a low noise amplifier, a band pass filter, and is collected by an Agilent 89600 Vector Signal Analyzer (VSA). The VSA can down-convert the RF signal to baseband and save the data in computer-readable format. The data collection process is shown in Figure 4.

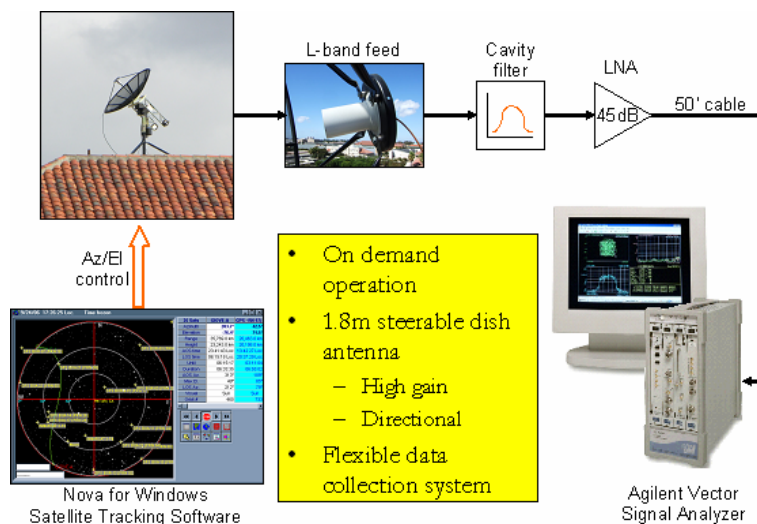


Figure 4. Block diagram of Stanford GNSS Monitoring System

## ACQUIRING AND TRACKING GIOVE-A SIGNALS

With all GIOVE-A broadcast PRN codes available, signals from the GIOVE-A test satellite are acquired and tracked with a multi-signal all-in-view GNSS software receiver implemented in MATLAB™ (Figure 5; [6] [7]). In addition to the Galileo signals, this receiver is also capable of signal acquisition and tracking of GPS C/A-code or pseudo-P-code (simulated signals only).

Acquisition is implemented as a parallel code-phase search using FFT-based processing. Several milliseconds of data are combined to increase weak-signal sensitivity or to provide more accurate estimates of carrier Doppler frequency, although at a trade-off in execution time.

The multi-signal GNSS software receiver is originally designed for GPS signals, so it handles the PRN codes of 1 msec. However, the Galileo codes can be a few milliseconds long, for example the L1-B code is 4 msec, the L1-C code is 8 msec and the E6-C code is 2 msec. A quick-fix is to overlay 4ms or 8ms of code onto a 1ms segment, and suffer the cross-correlation noise. It is also possible to break the 4ms or 8ms codes into four or eight 1ms chunks, and treat the acquisition problem as looking for those 1ms-long sequences in the stored data file.

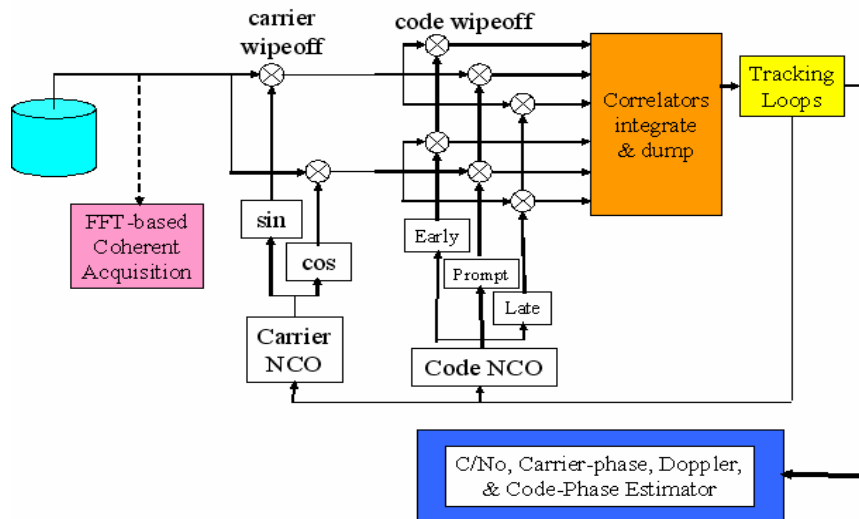


Figure 5. Software receiver block diagram

Immediately after acquisition, the code-phase and carrier-frequency estimates are used to initialize the code and carrier numerically-controlled oscillators (NCOs). The receiver refines the estimates of carrier frequency, carrier phase, and code phase through a succession of tracking modes, where the phase-lock and delay-lock loop noise bandwidths are successively reduced.

We load the raw GIOVE-A data collected through the SGMS dish and the Stanford SRI dish to our software receiver. We first pass the data into the acquisition module.

Figure 6 shows the acquisition and tracking results of the GIOVE-A L1 signal. For brevity, we only show the result for L1-B code, but the tracking results for L1-C are nearly identical. The 3-D acquisition plot on the left shows the normalized correlation function output as a function of code phase on one axis and carrier Doppler frequency on the other axis. We read the code-phase and Doppler estimate based on the location of the main peak in the code phase and Doppler domain. We then feed the code-phase and carrier-frequency information to the tracking module as an initial estimate. The tracking output in the righthand plot in Figure 6 shows four subplots as follows, each as a function of elapsed tracking time along the horizontal axis:

- Upper-left: Phase Lock Loop (PLL) discriminator output in degrees
- Upper-right: Delay Lock Loop (DLL) discriminator output in meters
- Lower-left: carrier Doppler frequency estimate
- Lower-right: code-phase estimate with respect to the receiver's on-board millisecond counter

The GIOVE-A L1 signal is successfully tracked. The tracking process is settled within 500 msec.

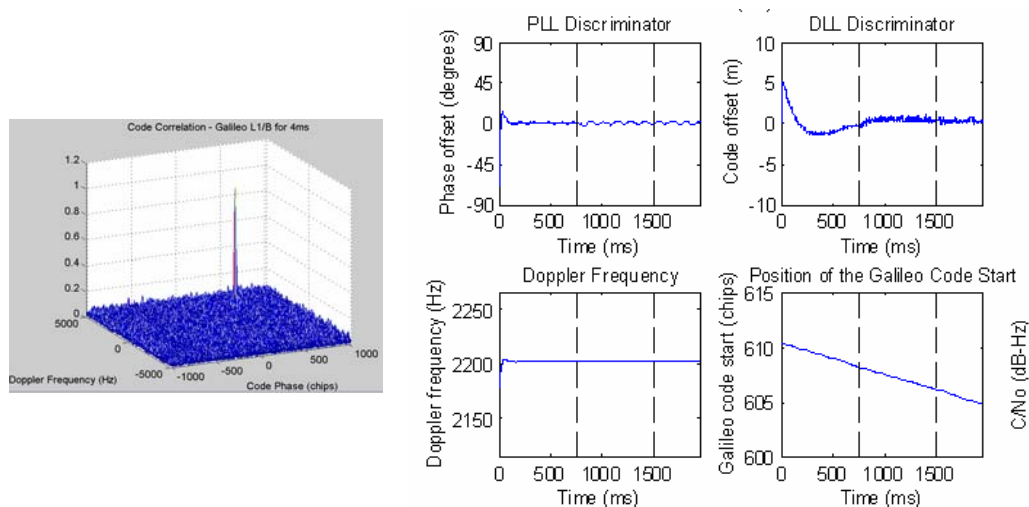


Figure 6. Acquisition and tracking results of GIOVE-A L1-B signal

Figure 7 shows the acquisition and tracking results of the GIOVE-A E6 signal. Again for brevity, we only show the result for E6-B code, but the results for tracking the E6-C code are very similar. The 3-D acquisition plot of the E6 signal shows a clearer peak and less noisy background than that of the L1 signal. This is because the E6 codes are longer and faster. The DLL and PLL both converge. This indicates the successful tracking of the GIOVE-A E6 signal.

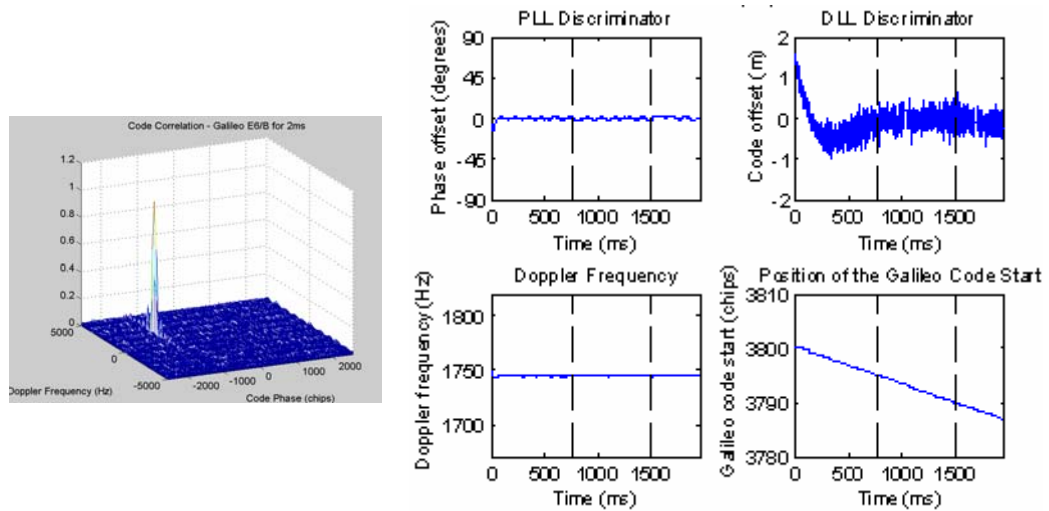


Figure 7. Acquisition and tracking results of GIOVE-A E6-B signal

The acquisition and tracking results of GIOVE-A E5 signal are shown in Figure 8. Although we can see an acquisition peak in the 3-D plot, it is very noisy. The correlation peak to next peak ratio (CPPR) is only 6.24dB. This indicates a low signal to interference plus noise ratio (SINR). The Doppler estimate is -700 Hz. Due to the low CPPR, this estimate can be inaccurate and can cause converging failure in the next tracking module. We then initiate the tracking mode by the rough estimate of the code-phase and carrier-frequency from the acquisition results. Unfortunately, the PLL and DLL are not locked. We observe excessive jumps in the estimates of phase offset and code offset. This is caused by inaccurate Doppler and code-phase output from the acquisition module. Doppler should be -450 Hz, but PLL incorrectly locks onto -700 Hz; poor aiding to DLL causes periodic large discriminator errors.

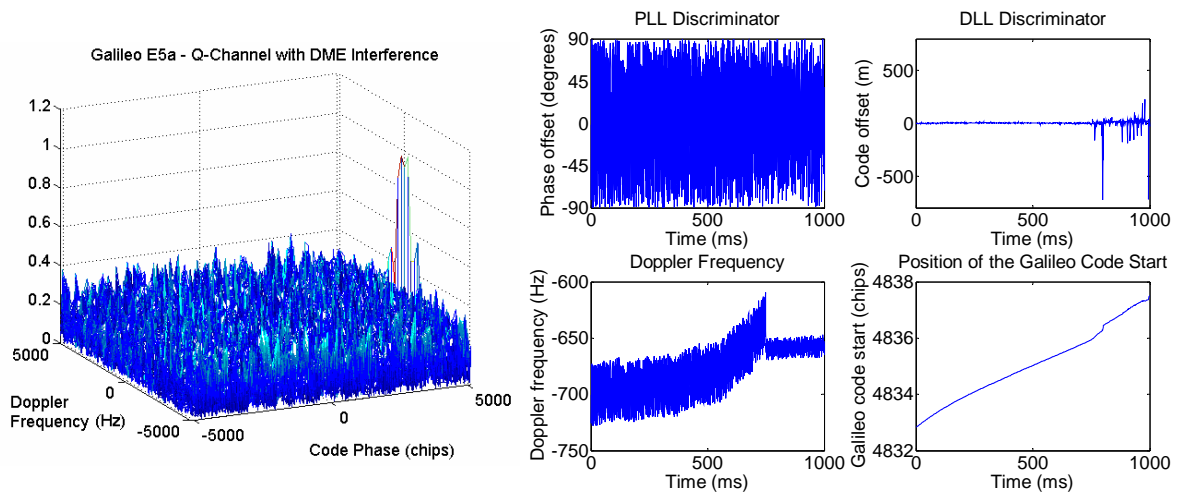


Figure 8. Acquisition and tracking results of GIOVE-A E5a signal

## DME INTERFERENCE

In the previous section, we have successfully acquired and tracked the GIOVE-A broadcast L1 and E6 signals. However, the acquisition and tracking results for E5 signal show a low SINR and the low SINR may cause tracking failure. The Galileo E5 band overlaps with the frequency band of existing aeronautical system pulsed emitters, especially Distance Measuring Equipment (DME) and Tactical Air Navigation (TACAN) systems. These navigation systems consist of an airborne interrogator and a ground-based transponder. DME/TACAN operate between 960 MHz and 1215 MHz in an Aeronautical Radionavigation Services (ARNS) band [5]. The DME/TACAN interference sources around Stanford University are illustrated in Figure 9. The DME/TACAN emitters of the airports marked in Figure 9 transmit pulses within Galileo E5 band, thus interfere with the E5 signal at receivers.

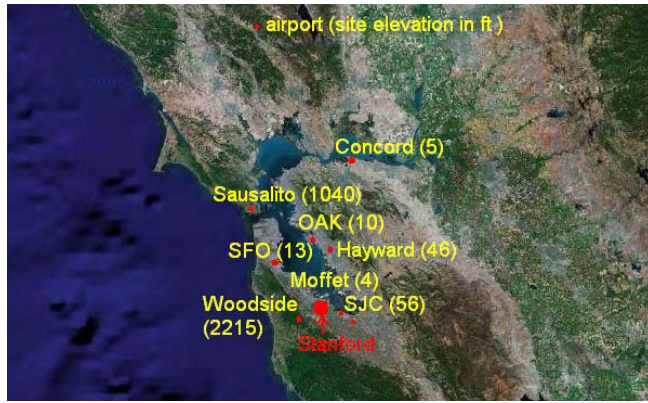


Figure 9. DME/TACAN interference sources around Stanford

Figure 10 shows the power spectral density of the E5a and E5b frequency bands. There are spikes in the frequency domain, corresponding to DME/TACAN beacons of nearby airports. The observed airports are Woodside, SJC, SFO, Sausalito, OAK, Moffet, as marked in Figure 10. The height of the spikes represents the received power of corresponding DME/TACAN signals. The received power is a function of the distance from the airports to the observing location, the elevation of the airports and the transmitted power level. Table 3 shows the longitude, latitude, site elevation, antenna height and transmitter power of the DME/TACAN beacons around Stanford University. Among these beacons, Woodside is the closest. It also has a high elevation. This explains why the Woodside spike is highest in the spectrum.

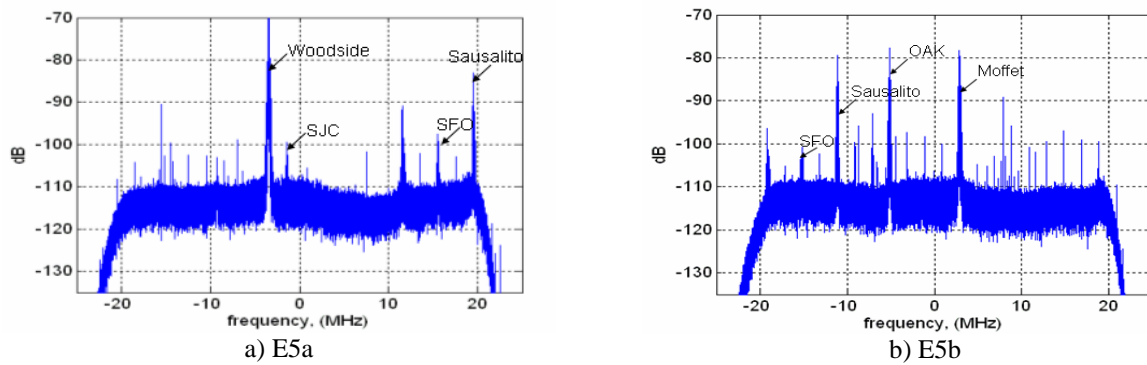


Figure 10. Power spectral density of E5a and E5b signals

Airport	Longitude	Latitude	Site elevation (ft)	Antenna height (ft)	Transmitter Frequency (MHz)
Woodside	37.39278	-122.28194	2215	16	1173
Moffet	37.43222	-122.05694	4	N/A	1210
SFO	37.61944	-122.37389	13	26	1192
SJC	37.37472	-121.94472	56	33	1175
OAK	37.72583	-122.22333	10	N/A	1202
Sausalito	37.85528	-122.5225	1040	N/A	1196

Table 3. Airports near Stanford, CA, USA

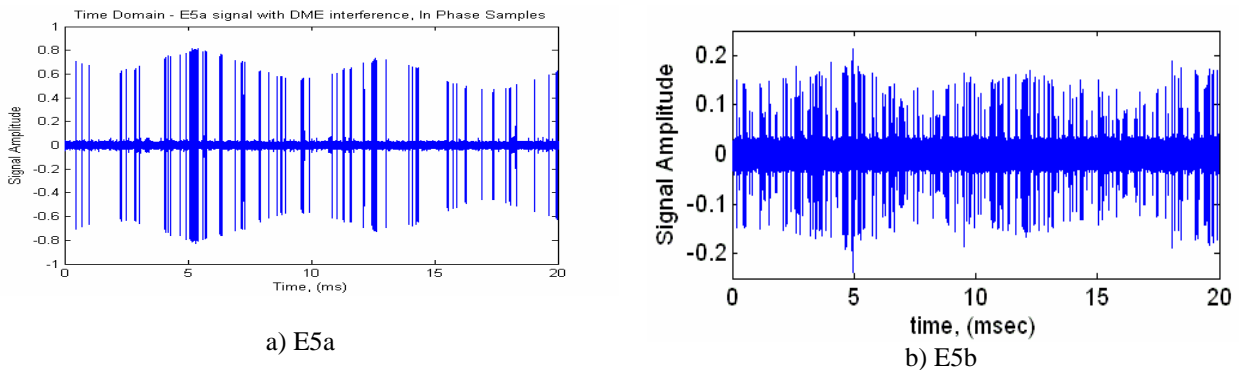


Figure 11. Time domain E5 signal with DME interference

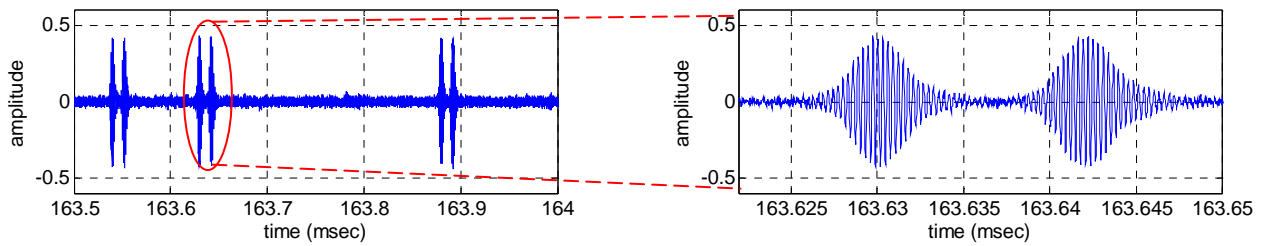


Figure 12. Time domain E5a signal with DME interference, zooming in

The received E5a signal in the time domain is illustrated in Figure 11 and Figure 12. The DME pulse amplitude is 5~100 times greater than the noise floor and the E5 signal is below the noise floor. DME interference occurs 10-14% of the time in this observation data set. The DME/TACAN interference is composed of pulse pairs with an inter-pulse interval of 12  $\mu$ s. If we zoom in, we can see the Gaussian shape of the pulses in Figure 12. The pulses have width of 3.5  $\mu$ sec and inter-pulse interval of 12  $\mu$ sec.

### DME INTERFERENCE MITIGATION TECHNIQUE

Digital pulse blanking has been discussed in [5]. It blanks the signal portions if their norm exceeds a certain threshold level as shown in Figure 13.

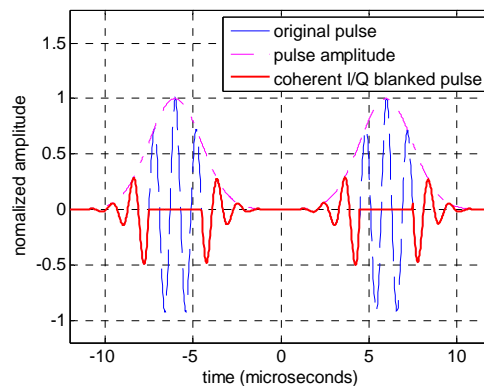


Figure 13. Digital pulse blanking

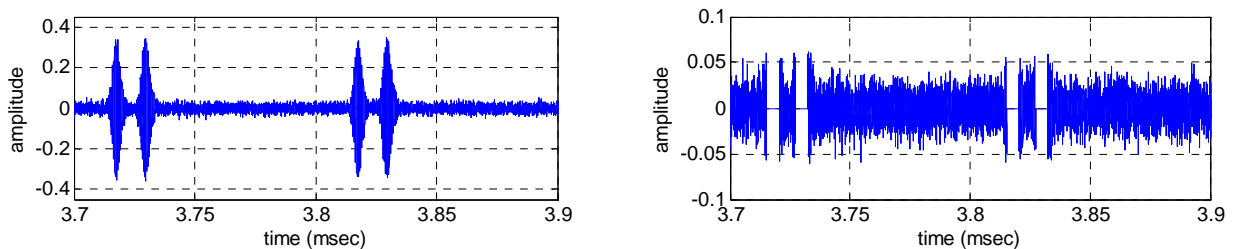


Figure 14. Time domain E5a signal before/after digital pulse blanking

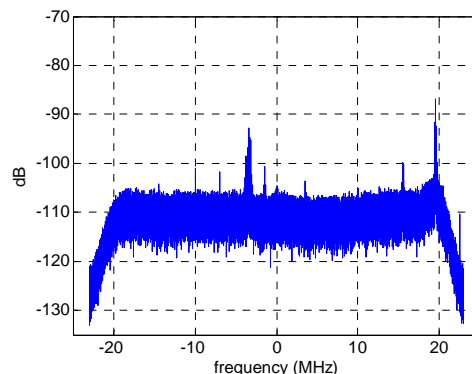


Figure 15. E5a power spectral density estimate, after digital pulse blanking

Figure 14 shows the time domain E5a signal before and after pulse blanking. Figure 15 shows the power spectrum. In this example, pulse blanking mitigates 22 dB of DME/TACAN interference, reducing the spikes from -70 dB to -92dB.

Digital pulse blanking is effective and simple to implement but does not completely eliminate all of the interference due to the bell shape of the DME/TACAN pulses. Their tails stretch below the noise floor, and thus cannot be removed by simple pulse blanking alone. This is the reason why we still see some small spikes remaining in the spectrum.

We further study the effectiveness of pulse blanking by using our software receiver. We applied pulse blanking before sending the raw data into the acquisition module. The 3-D plots in Figure 16 and 17 show the acquisition results for E5a-I and E5a-Q channels respectively. The integration time remains unchanged. This time, we see less noisy plots. The CPPR is increased from 6dB to 19dB by the pulse blanking technique. The Doppler estimate is now -420 Hz in both plots.

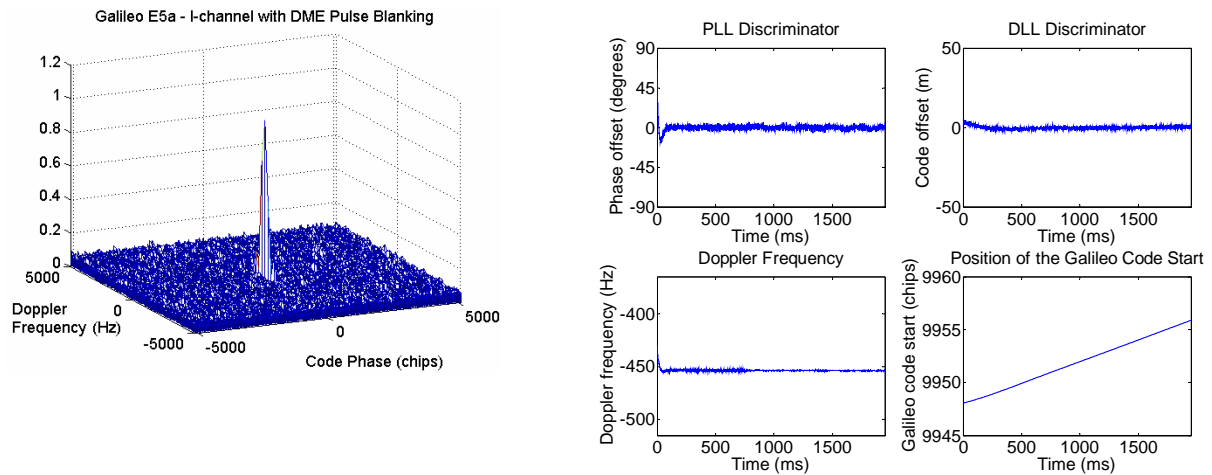


Figure 16. Acquisition and tracking results for GIOVE-A E5a-I signal with pulse blanking

Next, we initialize the tracking loops with the new code-phase and Doppler estimates. The tracking results of E5b-I and E5b-Q are shown in the right hand side plots in Figure 16 and 17 respectively. With digital pulse blanking, the PLL and DLL are locked. All tracking outputs converge, such as phase offset, code offset and Doppler frequency. The PLL and DLL discriminators settle within 100 msec. The Doppler frequency is locked at -450 Hz as shown in the tracking plots. Recall that in the non-pulse-blanking case, the Doppler estimate from the acquisition module is -700 Hz, which is wrong by 250 Hz. This makes the DLL and PLL incorrectly lock onto -650 Hz as shown in the lower-left plot in Figure 8, causing periodic large discriminator errors.

For brevity, we only show the acquisition and tracking results for E5a channel. The results for E5b are similar.

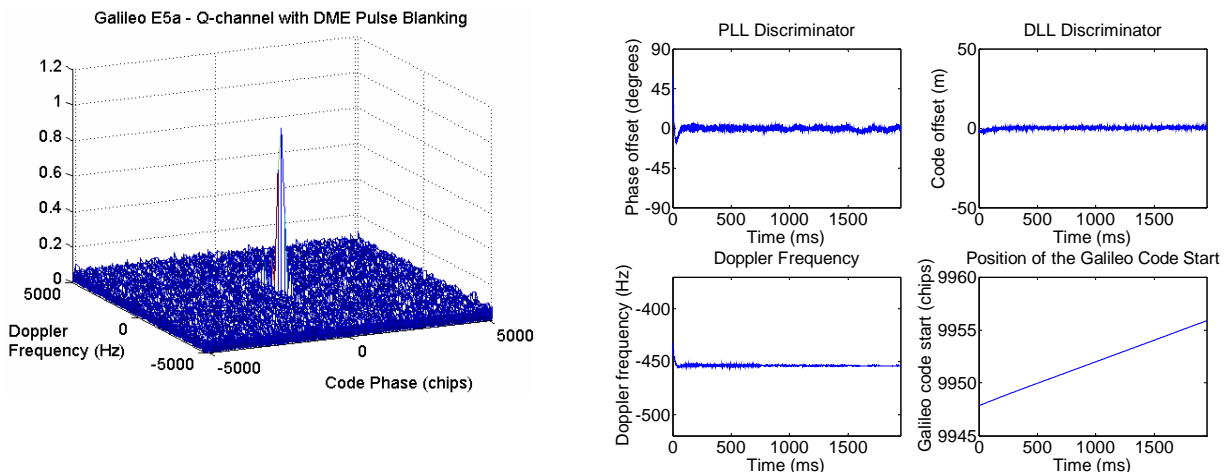


Figure 17. Acquisition and tracking results for GIOVE-A E5a-Q signal with pulse blanking

## COMPASS-M PRN CODES

On April 13 China launched the first middle earth orbiting (MEO) satellite in its Compass GNSS system, 21,550 kilometers or about 13,200 miles above the Earth. The spacecraft began transmitting signals on three frequencies (E2, E6 and E5b) within a few days. The initial orbital elements are inclination = 55.0°, eccentricity = 0.62, and mean motion = 3.84 orbits per day. [8]. We observed the transmitted Compass signal and collected the data. We processed the

data. The E2 signal is QPSK modulated. We have decoded the broadcast Compass E2 I-channel code. It has BPSK(2) modulation and is 2046 bits long. The first 100 code chips are shown in Figure 18. We not only decoded the code sequence, but also proved that the code is a 11-stage Gold code and derived the code generator polynomials and initial states as shown in Figure 19.

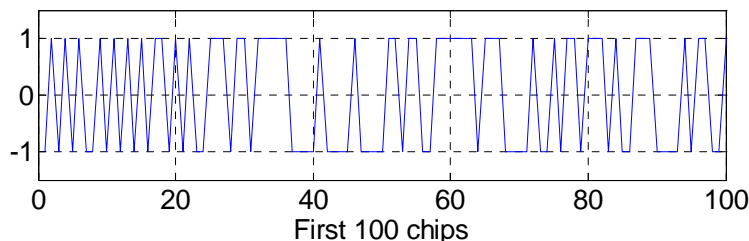


Figure 18. First 100 chips of Compass L1 signal

E2 I-channel code (2046 bits, 1msec, 11-stage Gold code)	
Polynomial_1	$X^{11}+X^{10}+X^9+X^8+X^7+X+1$
Initial State_1	[ 0 1 0 1 0 1 0 1 0 1 0 ]
Polynomial_2	$X^{11}+X^9+X^8+X^5+X^4+X^3+X^2+X+1$
Initial State_2	[ 0 0 0 0 0 0 0 1 1 1 1 ]

Figure 19. Compass L1 PRN code generator

## SUMMARY

This paper shows the acquisition and tracking results of GIOVE-A broadcast L1/E5/E6 signals using a multi-signal all-in-view software receiver. The L1 and E6 signals are tracked successfully. However, the E5 signal is exposed to pulsed interference from DME/TACAN emitters, which degrades the SINR ratio at the receivers, and caused tracking failure. We demonstrate that digital pulse blanking is an efficient and simple method to mitigate the DME/TACAN interference. The E5 signal was successfully tracked after the interference mitigation technique was applied to the raw data.

Recently, China launched the first middle earth orbiting (MEO) satellite in its Compass GNSS system in April 2007. The Compass E2 signal is observed. The E2 I-channel PRN code is decoded and proved to be a 11-stage Gold code. This paper also shows the Compass L1 code generator, including the code polynomials and the registrator initial states.

## ACKNOWLEDGEMENTS

The authors gratefully acknowledge the support of the Federal Aviation Administration under Cooperative Agreement 95-G-005. This paper contains the personal comments and beliefs of the authors, and does not necessarily represent the opinion of any other person or organization.

## REFERENCES

- [1]. Grace Xingxin Gao, Jim Spilker, Todd Walter, Per Enge and Anthony R Pratt, 'Code Generation Scheme and Property Analysis of Broadcast Galileo L1 and E6 Signals', ION GNSS conference, Fort worth, TX, USA, September 2006
- [2]. Grace Xingxin Gao, David S. De Lorenzo, Alan Chen, Sherman C. Lo, Dennis M. Akos, Todd Walter and Per Enge, 'Galileo Broadcast E5 Codes and their Application to Acquisition and Tracking', ION NTM conference, San Diego, CA, USA, January 2007
- [3]. European Space Agency, 'Successful launch of the Galileo Satellite: GIOVE-A, the First European Navigation Satellite in Space', December 28, 2005. Document can be found on-line at: <http://www.galileoju.com/doc/8541%20Press%20Release%20Successful%20Launch%20of%20GIOVE%20A.pdf>
- [4]. European Space Agency and Galileo Joint Undertaking, 'Galileo Open Service Signal In Space Interference Control Document (OS SIS ICD)', March 2, 2007. Document can be found on-line at: [http://www.giove.esa.int/page\\_index.php?menu=1000&page\\_id=59](http://www.giove.esa.int/page_index.php?menu=1000&page_id=59)
- [5]. Taehwan Kim, Joe Grabowski, 'Validation of GPS L5 Coexistence with DME/TACAN and Link-16 System', ION GNSS conference, Portland, OR, September 2003

- [5]. Frederic Bastide, Eric Chatre, Christophe Macabiau, Benoit Roturier, 'GPS L5 and Galileo E5a/E5b Signal-to-Noise Density Ratio Degradation Due to DME/TACAN signals: Simulation and Theoretical Derivation', ION NTM Conference, San Diego, CA, January, 2004
- [6]. D.S. De Lorenzo, J. Rife, P. Enge, and D.M. Akos, 2006, 'Navigation Accuracy and Interference Rejection for an Adaptive GPS Antenna Array,' Proc. ION GNSS 2006
- [7]. K. Borre, D.M. Akos, N. Bertelsen, P. Rinder, and S.H. Jensen, 'A Software-Defined GPS and Galileo Receiver: A Single-Frequency Approach', Birkhauser, 2006
- [8]. 'New Beidou Satellite', GPS World, April 27, 2007, can be found online at:  
<http://sidt.gpsworld.com/gpssidt/article/articleDetail.jsp?id=422958>